1510 *Inorg. Chem.* **2010**, *49*, 1510–1516
DOI: 10.1021/ic901872g

Inorganic Chemistry
Article

Characterization of the Order−Disorder Dielectric Transition in the Hybrid Organic−Inorganic Perovskite-Like Formate $Mn(HCOO)_3[(CH_3)_2NH_2]$

M. Sánchez-Andújar,[†] S. Presedo,[†] S. Yáñez-Vilar,[†] S. Castro-García,[†] J. Shamir,[‡] and M. A. Señarís-Rodríguez*,[†]

[†]*Dpto. Química Fundamental, Universidad de A Coruña, 15071 A Coruña, Spain, and* [‡]*Department of Inorganic and Analytical Chemistry, Hebrew University, Jerusalem, Israel*

Received September 22, 2009

We have found that the hybrid organic−inorganic perovskite-like formate $Mn(HCOO)_3[(CH_3)_2NH_2]$ shows a dielectric transition around 190 K. According to single crystal X-ray diffraction, the compound shows rhombohedral symmetry at room temperature and monoclinic symmetry at low temperature (100 K), and the main difference between both structures is that the $(CH_3)_2NH_2^+$ (DMA) cations are disordered in the high temperature phase but cooperatively ordered in the low temperature one. The vibrational spectra of this compound reveal that significant changes take place in the vibrations ascribed to the DMA cation (changes in the frequency of certain vibrations, splitting of particular vibrations, and changes in the intensities), while no significant changes have been observed in those attributed to the formate anion. On the basis of all this information, we attribute the origin of the dielectric transition to the dynamics of the DMA cations: above 190 K these cations can rotate inside the cubooctahedral cavity created by the $[Mn(HCOO)_3]^-$ framework, while for lower temperatures such rotation gets frozen, and their cooperative arrangement inside the cavities give rise to the observed dielectric transition.

Introduction

Hybrid materials that combine inorganic and organic components and that contain cavities and channels, the so-called metal organic frameworks (MOFs), have been extensively studied in the past decade in view of their interesting potential applications, for example, in catalysis and gas storage.[1,2]

In addition to nanoporous MOFs, more recently dense hybrid framework structures have also been discovered and are receiving increasing attention as they can display a wide range of interesting physical properties.[3,4]

In this context dielectric properties[5] and weak ferromagnetism[6] have been reported for different hybrid inorganic−organic materials with the perovskite architecture.

As it is well-known, the "conventional" perovskite structure, of general formula ABX_3 (A = lanthanide, alkaline-earth cations, etc.; B = transition metal cations; $X = O^{2-}$, S^{2-}, halide ions, etc.)[7] consists of a three-dimensional (3D) array of corner sharing $[BX_6]$ octahedra with the larger A cation occupying the 12-coordinated cubooctahedral cavities of the 3D network. Such structure is the basis of many transition metal mixed oxides with very outstanding properties such as high T_c superconductivity,[8] colossal magnetoresistance,[9] ferroelectricity,[7,10] charge ordering,[9] nonlinear optical behavior, catalytic properties,[11] and so on.

In addition to this "conventional" perovskite, there are some examples of hybrid inorganic−organic compounds with perovskite architecture. Up to now, all of them contain the formate ion $HCOO^-$ in the X site, the dimethylammonium cation $(CH_3)_2NH_2^+$ (DMA) in the A site, while different divalent cations, as Cu^{2+},[12] Mn^{2+}, Co^{2+}, Ni^{2+},[6] Zn^{2+},[5,13] and Mg^{2+} [14] can occupy the B site.

The recent discovery of a dielectric transition in the $Zn(HCOO)_3[(CH_3)_2NH_2]$ compound with perovskite architecture[5] has spurred the interest in this family of compounds and

*To whom correspondence should be addressed. E-mail: tonasr@udc.es. Phone: (+34) 981167000. Fax: (+34) 981167065.

(1) Yaghi, O. M.; O'Keeffe, M.; Ockwig, N. W.; Chae, H. K.; Eddaoudi, M.; Kim, J. *Nature* **2003**, *423*, 705.
(2) Fletcher, A. J.; Thomas, K. M.; Rosseinsky, M. J. *J. Solid State Chem.* **2005**, *178*, 2491.
(3) Cheetham, A. K.; Rao, C. N. R. *Science* **2007**, *318*, 58.
(4) Ferey, G. *Chem. Soc. Rev.* **2008**, *37*, 191.
(5) Jain, P.; Dalal, N. S.; Toby, B. H.; Kroto, H. W.; Cheetham, A. K. *J. Am. Chem. Soc.* **2008**, *130*, 10450.
(6) Wang, X. Y.; Gan, L.; Zhang, S. W.; Gao, S. *Inorg. Chem.* **2004**, *43*, 4615.
(7) Galasso, F. S. *Structure, properties and preparation of perovskite-type compounds*; Pergamon Press: Oxford, 1969.
(8) Rao, C. N. R.; Gopalakrishnan, J. *New Directions in Solid State Chemistry*; Cambridge University Press: Cambridge, 1997.
(9) Rao, C. N. R.; Raveau, B. *Charge Ordering and Related Properties of Manganese Oxide*; World Scientific: Singapore, 1998.
(10) Lines, M. E.; Glass, A. M. *Principles & applications of Ferroelectric & related materials*; Oxford University Press: New York, 2001.
(11) Tejuca, L. G.; Fierro, J. L. G. *Properties and applications of perovskite-type oxides*; CRC Press: Boca Raton, FL, 1992.
(12) Sletten, E.; Jensen, L. H. *Acta Crystallogr., Sect. B* **1973**, *29*, 1752.
(13) Clausen, H. F.; Poulsen, R. D.; Bond, A. D.; Chevallier, M. A. S.; Iversen, B. B. *J. Solid State Chem.* **2005**, *178*, 3342.
(14) Rossin, A.; Ienco, A.; Costantino, F.; Montini, T.; Di Credico, B.; Caparoli, M.; Gonsalvi, L.; Fornasiero, P.; Peruzzini, M. *Cryst. Growth. Des.* **2008**, *8*, 3302.

Published on Web 01/22/2010

has opened a new direction in the search for novel dielectric and even multiferroic materials.

In this context, the dielectric transition found in the Zn-compound was considered to be of paraelectric-antiferroelectric type in view of the similarities of the $\varepsilon_r(T)$ curve with that of other antiferroelectric materials.[5] Even more, Jain et al.[5] have proposed, on the basis of the room temperature crystal structure data, that such antiferroelectric phase transition is driven by ordering of the hydrogen atoms of the dimethylammonium cation,[5] even if direct proof of its origin has so far remained elusive.

In this work we focus in the related compound $Mn(HCOO)_3[(CH_3)_2NH_2]$, previously obtained by Wang et al. and that shows weak ferromagnetism ($T_c = 8.5$ K),[6] with a 2-fold purpose:

(1) We want to explore the dielectric properties and the possibility of an electrical ordering in this compound that, as indicated above, also shows magnetic properties and could thus show additional interesting multiferroic behavior.[15]

(2) We are interested in pursuing the origin of order−disorder transitions, and accompanying dielectric transitions, occurring in hybrid inorganic−organic compounds with perovskite-like structure.

In the course of the submission of this paper a short communication has been published[16] that claims the multiferroic nature of different dimethylamonium metal formates with M: Mn, Fe, Co, Ni. Our dielectric, crystallographic, and vibrational data supplement the information available for the Mn-compound and shed light on the origin of the observed dielectric transition.

Experimental Section

Materials. $MnCl_2 \cdot 4H_2O$ (99%, Aldrich), *N*,*N*-dimethylformamide (DMF) (99.8%, Panreac), absolute ethanol (Panreac), and formic acid (98%, Fluka) were commercially available and used as purchased without further purification. A reagent amount of deionized water was also used in the synthesis.

Synthesis. The synthetic route used here is an adaptation of the previously reported one for the preparation of the $Mg(HCOO)_3[(CH_3)_2NH_2]$ compound.[14] In a typical experiment, 20 mL of DMF, 1 mL of ethanol, 1 mL of water, 0.3 mL of formic acid, and 2.1 g of $MnCl_2 \cdot 4H_2O$ were heated 48 h in a Teflon lined autoclave at 140 °C. After slow overnight cooling, colorless cubic-like crystals were obtained. They were collected, washed with ethanol, and dried at room temperature.

In contrast with the synthetic method previously used by Wang et al.[6] to prepare the Mn-compound, that involved a hydrothermal treatment followed by a slow evaporation, the one described here allows to obtain this compound in one single step.

Crystallographic Structure Determination. Single-crystal data sets of the sample were collected at 295 and 100 K in a Bruker-Nonius x8 ApexII X-ray diffractometer equipped with a CCD detector and using monochromatic $MoK\alpha_1$ radiation (λ = 0.71073 Å). A suitable crystal was chosen and mounted on a glass fibber using instant glue. For the 100 K set, the crystal temperature was maintained using a cold stream of nitrogen from a Kyroflex cryostream cooler. The data integration and reduction was performed using the Apex2 V.1.0−27 (Bruker Nonius, 2005) suite software. The intensity collected was corrected for Lorentz and polarization effects and for absorption by semiempirical methods on the basis of symmetry-equivalent data using SADABS (2004) of the suite of software. The structures were solved by the direct method using the SHELXS-97[17] program and were refined by least-squares method on SHELXL-97.[18]

To solve the structure at 295 K, anisotropic thermal factors were employed for the non-H atoms. The hydrogen atoms of the formate ions were found in the Fourier map, and their coordinates and isotropic thermal factors were refined. Meanwhile, the H-atoms of the DMA could not be found or added, presumably because of the disordered arrangement of this cation (see below).

To solve the structure at 100 K, anisotropic thermal factors were also employed for non-H atoms. At this temperature, the hydrogen atoms of the NH_2^+ group of the DMA cation were found in the Fourier map, and their coordinates and isotropic thermal factors were also refined; the rest of the hydrogen atoms of the DMA were introduced at idealized positions.

In addition, the compound was studied by X-ray powder diffraction (XRPD) at room temperature in a Siemens D-5000 diffractometer using CuKα radiation (λ = 1.5418 Å). The XRPD pattern was analyzed by the Le Bail profile analysis using the GSAS software.[19]

Dielectric Properties. The complex dielectric permittivity, $\varepsilon_r = \varepsilon'_r - i\varepsilon''_r$, of the cold-press pelletized sample was measured as a function of frequency and temperature with a parallel-plate capacitor coupled to a Solartron 1260A Impedance/Gain-Phase Analyzer, capable of measuring in the frequency range 10 μHz to 32 MHz using an amplitude of 1 V. The capacitor was mounted in a Janis SVT200T cryostat refrigerated with liquid nitrogen, and with a Lakeshore 332 incorporated to control the temperature from 78 K up to 300 K. The data were collected upon heating the sample at an approximate rate of 0.8 K/min. Pellets with an area of approximately 300 mm^2 and thickness of approximately 0.6 mm were prepared to fit into the capacitor, and gold was sputtered on their surfaces to ensure a good electrical contact with the electrodes. The impedance analysis software SMART (Solartron Analytical) was used for data acquisition and processing.

Raman Studies. Powder Raman spectra were measured both at 300 K and at 75 K with a Jobin Yvon Typ V 010 Labram single grating spectrometer, equipped with a double super razor edge filter and a Peltier cooled CCD camera. Spectra were recorded over the wavenumber range of 50−3200 cm^{-1}, with a resolution of 1 cm^{-1}, in quasi-backscattering geometry using the linearly polarized 632.817 nm line of an He/Ne gas laser (with power less than 1 mW), focused to a 15 μm spot through a 20× microscope objective onto the sample surface. A Helium-microcryostat from Cryovac was used for the low temperature studies.

Results

Dielectric Properties. Panels a and b in Figure 1 show the temperature dependence of the real part of the complex dielectric permittivity ε'_r (the so-called dielectric constant) and of the dielectric losses (tanδ). As it can be seen, for measuring frequencies of 1 and 10 kHz the dielectric constant shows a sharp increase from ∼185 to 190 K, temperature interval in which the loss tangent goes through a maximum. In addition, for $T > 190$ K ε'_r is seen

(15) Cheong, S. W.; Mostovoy, M. V. *Nat. Mater.* **2007**, *6*, 13.

(16) Jain, P.; Ramachandran, V.; Clark, R. J.; Zhou, H. D.; Toby, B. H.; Dalal, N. S.; Kroto, H. W.; Cheetham, A. K. *J. Am. Chem. Soc.* **2009**, *131*, 13625.

(17) Sheldrick, G. M. *SHELXS-97: Program for Crystal Structure Resolution*; University of Göttingen: Göttingen, Germany, 1997.

(18) Sheldrick, G. M. *SHELXL-97: Program for Crystal Structure Analysis*; University of Göttingen: Göttingen, Germany, 1997.

(19) Larson, A. C.; von Dreele R. B. *General Structure Analysis System* (*GSAS*); Los Alamos National Laboratories: Los Alamos, NM, 1990; Report LAUR, pp 86−748.

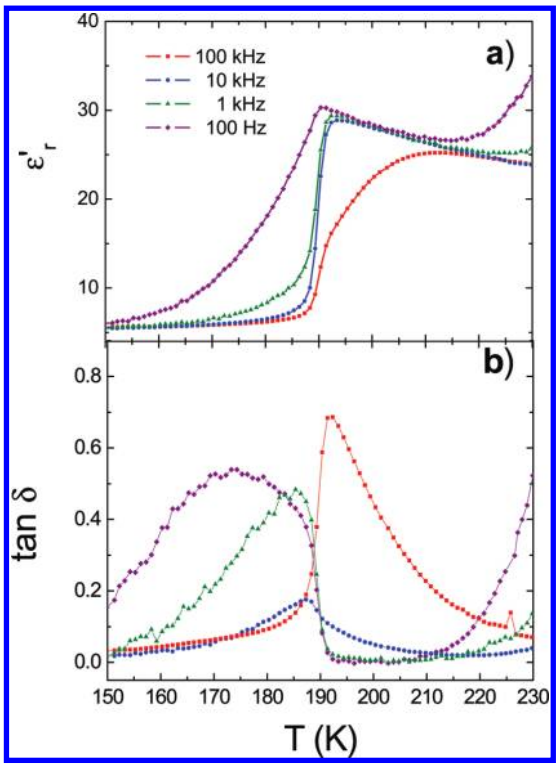

Figure 1. Temperature dependence of (a) the dielectric constant, ε'_r, and (b) the dielectric losses, tan δ, of $Mn(HCOO)_3[(CH_3)_2NH_2]$ measured at different frequencies (1 Hz $\leq \nu \leq$ 100 kHz).

to decrease as temperature increases further following the typical trend of a paraelectric behavior.

For lower measuring frequencies such dielectric transition is seen to occur over a wider temperature range, see Figure 1, while for higher frequencies (ν = 100 kHz) the whole transition is shifted to slightly higher temperatures.

It should be indicated that the DSC results confirm the presence of a phase transition in the temperature interval $\Delta T \sim 180-190$ K (see the Supporting Information, Figure S1). Interestingly, the exact temperature at which it is seen to take place markedly depends on the heating rate, revealing the influence of kinetics in the observed transition.

Structural Studies. The single-crystal X-ray studies carried out above and below the dielectric transition, namely, at 295 and 100 K, show that this compound presents different structures at those two temperatures. At 295 K, the sample crystallizes in the $R\bar{3}c$ non-centrosymmetric space-group, while at low temperature it crystallizes in the Cc centrosymmetric space-group. In the following paragraphs we will describe the main characteristics of both structures, focusing on that obtained at low temperature ($T < T_t$) that to our best knowledge is the first time that it is described for this type of compounds.

Room Temperature Structure. Although the room temperature crystal structure of $Mn(HCOO)_3[(CH_3)_2NH_2]$ is already known,[6] as well as those of the other formates with Cu,[12] Co, Ni,[6] Zn,[5,13] Mg[14]), we have studied it and refer here to its main characteristics as reference to compare with the low temperature results.

In this context it should be indicated that our structural data, summarized in Tables 1 and 3 and in Figure 2, are in full agreement with those reported in the literature.[6]

Table 1. Data Collection, Cell and Refinement Parameters from the Single Crystal X-ray Diffraction Study Carried out at T = 295 K

empirical formula	$MnC_5H_{11}NO_6$
formula weight	236.09
temperature/K	295(2)
wavelength/Å	0.71069
crystal system	$R\bar{3}c$
unit cell dimensions	
a/Å	8.3371(8)
c/Å	22.909(5)
volume/Å^3	1379.0(3)
Z	6
density(calculated)/ g/cm^3	1.706
absorption coefficient/ mm	1.435^{-1}
F(000)	726
crystal size/mm	0.19 × 0.09 × 0.06
crystal color	Colorless
θ range for data collection	3.33 to 28.25
index ranges	$-10 \leq h \leq 11$
	$-11 \leq k \leq 11$
	$-30 \leq l \leq 25$
reflections collected	4154
unique reflections	380 [R(int) = 0.0391]
completeness to θ = 28.25/%	99.2
refinement method	full-matrix least-squares on F^2
data/restraints/parameters	380/0/28
goodness of fit on F^2	1.188
final R index [$I > 2\sigma(I)$]	R_1 = 0.0288
	wR_2 = 0.0798
R index (all data)	R_1 = 0.0347
	wR_2 = 0.0838
largest diff peak and hole/e Å^3	0.37 and −0.21

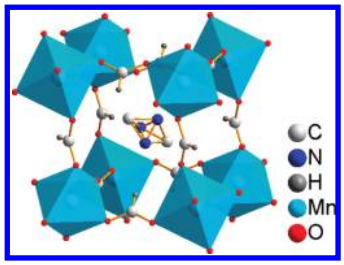

Figure 2. Conventional perovskite structure view of $Mn(HCOO)_3[(CH_3)_2NH_2]$ at room temperature.

At room temperature, this compound shows a distorted perovskite-like structure with rhombohedral symmetry ($R\bar{3}c$ space group). The asymmetric unit of the structure contains one independent metal cation, one $HCOO^-$ formate group bonded to the metal cation, and one disordered DMA cation $(CH_3)_2NH_2^+$. As a result, each metal cation is connected to its six metals nearest neighbors through six formate bridges (Figure 2) in an octahedral environment where the Mn−O distance is 2.19 Å (see Table 3). Most interestingly, the DMA cations that occupy the cubooctahedral cavities are disordered with nitrogen apparently existing in three different possible positions, as it has also been described for all the known perovskite-like formates[6] (Figure 2). Also, the distance between the N atom of DMA and the O atoms of the closest formate anion ($d \sim 2.93$ Å) is short enough to allow the presence of a bridging H-bond between these two atoms, even if the H atoms could not be located because of the disorder.

The LeBail refinement of the XRPD data confirms that the obtained Mn-compound is single phased, showing good agreement between the experimental data and the proposed model for the fitting (see Figure 3).

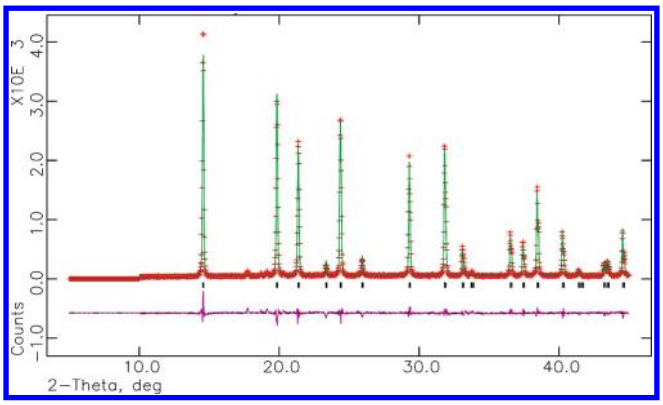

Figure 3. LeBail refinement of the XRPD pattern at room temperature. Key: observed data (+) and calculated profile (solid line); the difference plot is drawn below the profile. Tick marks indicate peak positions of the $Mn(HCOO)_3[(CH_3)_2NH_2]$ sample.

Table 2. Data Collection, Cell, and Refinement Parameters from the Single Crystal X-ray Diffraction Study Carried out at T = 100 K

empirical formula	$MnC_5H_{11}NO_6$
formula weight	236.09
temperature/K	100(2)
wavelength/Å	0.71069
crystal system	*Cc*
unit cell dimensions	
a/Å	14.345(2)
b/Å	8.323(1)
c/Å	8.879(1)
β	120.694(2)
volume/Å^3	911.6(2)
Z	4
density(calculated)/ g/cm^3	1.720
absorption coefficient/ mm^{-1}	1.447
F(000)	484
crystal size/ mm	0.19 × 0.09 × 0.06
crystal color	Colorless
θ range for data collection	3.30 to 27.23°
index ranges	$-19 \le h \le 19$
	$-10 \le k \le 11$
	$-10 \le l \le 11$
reflections collected	4888
unique reflections	1947 [*R*(int) = 0.0337]
completeness to θ = 27.23 /%	99.6
refinement method	full-matrix least-squares on F^2
data/restraints/parameters	1947/2/127
goodness of fit on F^2	1.018
final R index [$I > 2\sigma(I)$]	R_1 = 0.0370
	wR_2 = 0.0837
R index (all data)	R_1 = 0.0483
	wR_2 = 0.0901
largest diff peak and hole/ e Å^3	0.745 and −0.481
Flack parameter	0.46 (4) racemic twin

Crystallographic Structure at 100 K. The low temperature data can be indexed in a monoclinic system and in principle in two possible space groups: *C*2/*c* (centrosymmetric) and *Cc* (non-centrosymmetric).

When trying to refine the structure in the *C*2/*c* space group, a number of drawbacks were encountered: the agreement factors were worst than in the case of using the space group *Cc*; the results suggested disordered DMA cations with the nitrogen atom apparently in two different positions and with two very different N−C bond lengths (1.34 Å and 1.63 Å) that make no chemical sense for such cation. Because of all these incongruities, the space group (*C*2/*c*) was ruled out.

Meanwhile, the low temperature structure could be satisfactorily solved in the *Cc* space group with cell parameters of a = 14.345(2) Å, b = 8.323(1) Å, c = 8.879(1) Å, and β = 120.694(2)°. The most relevant structural information is summarized in Tables 2 and 3 that also includes bond lengths and bond angles. In addition, we have to note that the crystal is twinned and that a racemic twin is observed at low temperature, with a Flack parameter of 0.46(4).

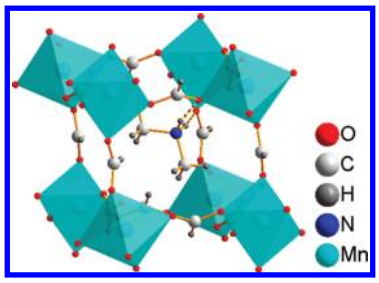

Figure 4. Main features of the crystal structure of $Mn(HCOO)_3[(CH_3)_2NH_2]$ at 100 K shown on the basis of the conventional perovskite structure view. Dash lines indicate H-bonds between the N atoms of DMA and O atoms of formate ions.

Table 3. Selected Bond Lengths and Bond Angles of $Mn(HCOO)_3[(CH_3)_2NH_2]$ at T = 295 K and T = 100 K

Bond Lengths			
T = 295 K		T = 100 K	
Mn environment			
Mn−O1	2.188 (1)	Mn−O1	2.184(4)
		Mn−O2	2.193(4)
		Mn−O3	2.162(4)
		Mn−O4	2.148(4)
		Mn−O5	2.198(4)
		Mn−O6	2.210(4)
Formate			
C1−O1	1.241(2)	C1−O1	1.254(8)
		C1−O5	1.246(8)
		C2−O2	1.251(6)
		C2−O6	1.253(6)
		C3−O4	1.252(6)
		C3−O3	1.260(6)
DMA			
C2−N1	1.431(7)	C4−N1	1.497(8)
		C5−N1	1.476(8)
Bond Angles			
T = 295 K		T = 100 K	
Formate			
O1−C1−O1	126.5(3)	O5−C1−O1	125.1(3)
		O6−C2−O2	124.2(4)
		O4−C3−O3	127.3(5)
DMA			
C2−N1−C2	118.7(7)	C5−N1−C4	112.4(5)

Some remarkable results come out from the structure resolution at 100 K:

(i) The first one is the ordering of the DMA cations inside the cubooctahedral cavity, as it can be observed in Figure 4. The N atom of the DMA cation sits in a single crystallographic position, in contrast with the room temperature structure.

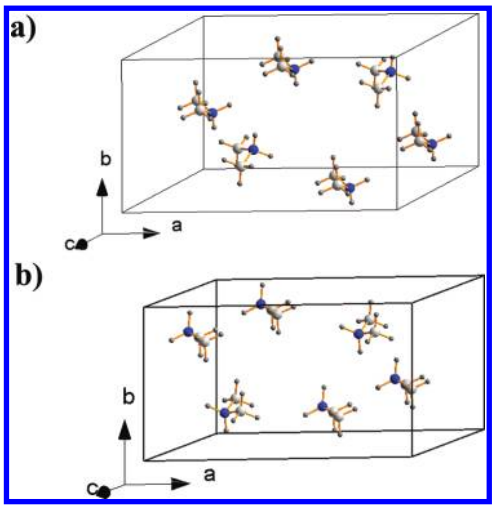

Figure 5. Cooperatively ordered arrangement of the DMA cations inside the unit cell corresponding to enantiomer (a) *one* and (b) *two*. The $Mn(HCOO)_3^-$ framework has been removed from the picture for a clearer view of the DMA cations.

Also, the distance between the N atom of DMA and the O atoms of the closest formate anion ($d \sim 2.83$ Å) is shorter than at room temperature, and well-defined and permanent N−H···O hydrogen bonds are present at 100 K (see Figure 4). Even more, the ordering of the DMA cations inside the cubooctahedral cavities is cooperative in the structure, so that the two enantiomers show an arrangement of the DMA cations in opposite directions as shown in panels a and b of Figures 5.

(ii) Another interesting feature is that at 100 K the $[Mn(HCOO)_3]^-$ framework is distorted: the Mn cations are in a distorted octahedral environment with six different Mn−O distances (see Table 3), and six slightly different C−O distances are detected for the formate anions. This is in contrast to the room temperature phase, which shows a regular octahedral Mn environment and only one C−O distance for all the formate ions (see Table 3).

Vibrational Studies. The Raman spectra obtained at low temperature (75 K) and at high temperature (300 K) are shown in Figures 6, 7 and 8. The corresponding IR spectra can be seen in the Supporting Information, Figure S2.

The observed frequencies (in cm^{-1}) of these vibrational spectra, that are in good agreement with data of the literature including suggested assignments that were mostly based on those sources,[20−22] are summarized in the Supporting Information, Table 4. However, these assignments are not always simple and straightforward as the vibrations of the NH_2^+ and the CH_3 groups may overlap and are indeed very close to one another. Yet, the observed frequencies of the stretching vibrations of the N−H bonds in amines are usually higher than those of the C−H ones.

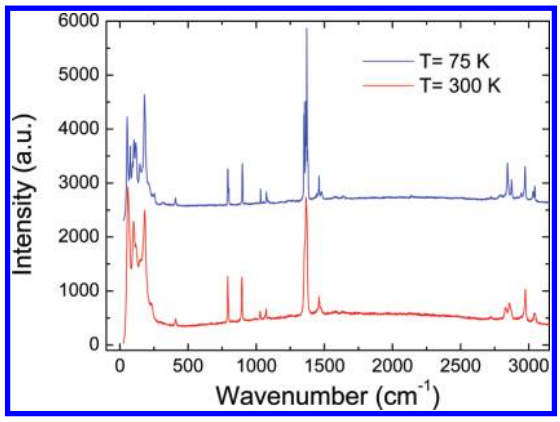

Figure 6. Raman spectra of $Mn(HCOO)_3[(CH_3)_2NH_2]$ recorded at low temperature (75 K) and at high temperature (300 K) corresponding to the whole spectral range 50−3200 cm^{-1}.

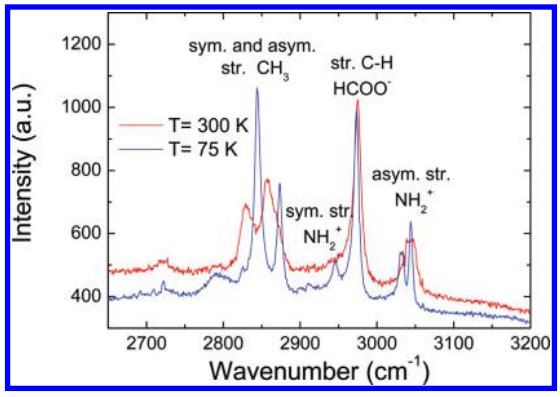

Figure 7. Detail of the Raman spectra results corresponding to the high wavenumber region (T = 75 and 300 K).

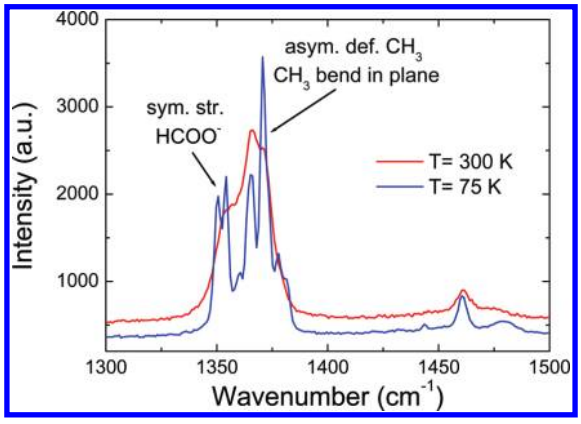

Figure 8. Detail of the Raman spectra corresponding to the region 1300−1500 cm^{-1} (T = 75 and 300 K).

Three types of A−H vibrations are present in dimethyl amine formate namely, NH_2^+, CH_3, and $HCOO^-$. Very interestingly, spectral changes as a result of temperature changes are observed in the vibrations of the CH_3 and NH_2^+ groups in the DMA cation but not of the C−H stretch of the $HCOO^-$ anion. Indeed in the stretching region of the spectra, the Raman frequency at 2974 cm^{-1} remains consistent at both temperatures and is thus assigned as the stretching vibration of the C−H of the formate anion which is the framework of this compound.

(20) Bator, G.; Baran, J.; Jakubas, R.; Sobczyk, L. *J. Mol. Struct.* **1998**, *450*, 89.
(21) Ebsworth, E. A. V.; Sheppard, N. *Spectrochim. Acta* **1959**, *13*, 261.
(22) Ito, K.; Bernstein, H. J. *Can. J. Chem.* **1956**, *34*, 170.

On the other hand, significant changes take place in the stretching vibrations of both the NH_2^+ and CH_3 of the DMA cation (see also the Supporting Information, Table 4):

(i) The asymmetric stretching vibration of the NH_2^+ group in the high temperature phase is observed as a broadband between 3049 and 3040 cm^{-1} while at low temperature it is split into two sharp lines at 3044 and 3033 cm^{-1}. In addition, a new line is observed in this region at 2946 cm^{-1} which may be the symmetric stretching vibration of the NH_2^+ group (see Figure 7).

(ii) The asymmetric stretching vibration of the CH_3 group at 2857 cm^{-1} in the high temperature phase shifts to a sharp line at a higher frequency at 2874 cm^{-1} when lowering the temperature. Similarly, the symmetric stretching vibration of the CH_3 group at 2826 cm^{-1} in the high temperature shifts to a sharp line at 2844 cm^{-1} when lowering the temperature. In addition, the relative intensities of these two vibrations are reversed with the change of the temperature. At 300 K the asymmetric stretch is more intense than the symmetric stretch while at low temperature it is just the opposite (see Figure 7).

(iii) In the region of deformation vibrations similar effects are noticed. In the high temperature phase a very broad band is observed between 1370 and 1350 cm^{-1} which has two shoulders at 1370 and 1350 cm^{-1} and is split into numerous sharp lines when lowering the temperature (see Figure 8). Tentative assignments are made, namely, 1381 and 1371 cm^{-1} as asymmetric deformations of the CH_3 group, and 1378 cm^{-1} may be assigned as CH_3 bend in plane. Meanwhile, that the band at 1351 cm^{-1} corresponds to the symmetric stretch of the carbon−oxygen bonds in the formate anion and does not significantly change with temperature, as it occurs with its asymmetric stretch that is observed at 1585 cm^{-1}.

The frequencies below 407 cm^{-1} are basically libration vibrations of the crystal and are much more difficult to assign.

Discussion and Conclusions

The compound $Mn(HCOO)_3[(CH_3)_2NH_2]$ shows a marked dielectric transition around 190 K, which is a result that is in full agreement with that very recently reported by Jain et al. for this same compound.[16] The shape and characteristics of this transition are also very similar to that shown by $Zn(HCOO)_3[(CH_3)_2NH_2]$,[16] although in the Zn compound this takes place at lower temperature (approximately at 160 K).

As in this latter case, the shape of the $\varepsilon'_r(T)$ curves around 190 K remind of those typical for paraelectric to antiferroelectric transitions, such as that of ADP at 148 K.[23] Therefore, such transitions have been catalogued as antiferroelectric ones. Nevertheless, they are also similar to those shown, for example, by alkylamonium halogenoantimonates (III) and bismuthates (III)[20,25,26] where a number of order−disorder phase transitions are related to the dynamics of the cations that rotate inside the cavities of the structure.

Jain et al. have proposed (initially for the dimethylamonium Zn-formate[5] and very recently for the equivalent Mn-compound[16]) that the observed dielectric anomaly is probably related to a classical paraelectric to antiferroelectric phase transition driven by the ordering of the H-atoms of the DMA cations at low temperature. Nevertheless, they could not provide direct proof for such origin as they were not able to solve the low temperature crystal structure because of the complex twinning of the crystals. Nevertheless, they detected splitting spots while collecting single crystal X-ray data at low temperature and shifting of the peaks while collecting synchrotron X-ray powder at low temperature, which evidenced the existence of a structural phase transition when cooling.[5]

Our $Mn(HCOO)_3[(CH_3)_2NH_2]$ crystals, although twinned could be resolved, and here we report the structural characteristics and vibrational spectra of this Mn-formate both at high and low temperature, results which permit to deepen the study of the origin of such a transition.

At room temperature, and as in the case of the Zn-compound, the DMA cations that sit in the cuboctahedral cavities of the perovskite-like structure are disordered with N apparently existing in three possible positions. This, in turn, would imply disordered N−H···O bonds between the DMA and the formate ions.

Meanwhile, according to the single crystal X-ray diffraction results, at 100 K the N atoms of the DMA cations occupy a single crystallographic site and in addition such DMA cations are cooperatively ordered within the crystal following the pattern shown in Figure 5.

This situation, again, has a strong resemblance with that found in ammonium and other small size alkylamonium halogenoperovskites[24] and alkylamonium halogenoantimonates(III) and bismuthates(III)[20,25,26] that present a high temperature phase characterized by a considerable degree of freedom for rotational motion of alkylamonium cations inside the cavities defined by the $[MX_6]^{n-}$ octahedra. Meanwhile, diminution and freezing of their reorientational motion on lowering the temperature gives rise to low temperature polymorphs consisting in ordered phases of different nature (pyroelectric, ferroelectric, ferroelastic, etc.).[20,24]

As done in the case of such compounds, we have recorded and analyzed the vibrational spectra of $Mn(HCOO)_3[(CH_3)_2NH_2]$.

We have found that various spectral changes take place in the vibrations ascribed to the DMA cation, changes in the frequency of certain vibrations, splitting of particular vibrations, and changes in the intensities, while no significant changes have been observed in those attributed to the formate anion. Specially notorious are the changes observed in the stretching vibrations of both its NH_2^+ and its CH_3 groups.

In this context, it is worth noting that Bator et al.[20] in their studies of the vibrational spectra of alkylamonium halogenoantimonates(III) and bismuthates(III), combined

(23) Gough, S. R.; Ripmeester, J. A.; Dalal, N. S.; Reddoch, A. H. *J. Phys. Chem.* **1979**, *83*, 664.

(24) Rubín, J.; Bartolomé, J.; Laguna, M. A.; Sanjuán, M. L. *Physica B* **1996**, *217*, 227.

(25) Sobczyk, L.; Jakubas, R.; Zaleski, J. *Pol. J. Chem.* **1997**, *71*, 265.

(26) Latanowick, L.; Medycki, W.; Jakubas, R. *J. Phys. Chem. A* **2005**, *109*, 3097.

with NMR spectroscopic results, have claimed that the stretching frequency is the most objective parameter describing a perturbation caused by the proton-accepting surroundings. Also, they describe for such compounds the splitting of the Raman and IR bands ascribed to the vibration of the DMA cation on passing from the high temperature phase to the low one: Above the transition temperature single broad bands are observed for the corresponding vibrational modes in the Raman and IR spectra as the cations, because of rotation, are subjected to an averaged field. Meanwhile, below the phase transition and as the cations are captured at a certain orientation, the vibrations of the cation are usually observed to be split into multiple sharp lines at lower or higher frequencies.

Therefore the here reported changes in the vibrational spectra of $Mn(HCOO)_3[(CH_3)_2NH_2]$ above and below the transition temperature can be taken as indication of changes in the degree of rotation of the DMA cations inside the perovskite cavity.

On the basis of all this information, we can rationalize the dielectric response of this compound as follows:

The paraelectric behavior observed for $T > 190$ K would be due to the fact that at those temperatures the DMA cations are not static but would be rotating inside the cavity, which is big enough to allow for such a process. Such rotation would take place around an axis that passes through the two C atoms of the DMA, a result that would also justify why at room temperature and according to X-ray diffraction the N atoms are 3-fold disordered, with the two carbon atoms lying in the 3-fold axis (see the Supporting Information, Figure S3). This rotation can occur because at those temperatures the thermal energy is able to overcome the strength of the hydrogen bonds that keep the DMA cations weakly bonded inside the Mn-formate framework. As a consequence, the electrical dipoles associated to the DMA cations would average in different directions upon rotation, and a paraelectric behavior would be observed.

As temperature decreases, the rotation of the DMA cations slows down and, as a consequence, ε'_r increases.

At around 190 K the disorder−order transition associated to the freezing of the molecular rotation of the DMA cations takes place: below that temperature the DMA cations can no longer rotate and have their positions fixed inside the cavities and are linked to the O-atoms of the formate anions by permanent N−H···O bonds. Simultaneously, significant changes in the $[Mn(HCOO)_3]^-$ framework occur, and a change in the symmetry of the crystal occurs.

As a result, a sharp drop in the dielectric constant takes place.

Even more, according to the XR diffraction results the order of the DMA cations within the Mn-formate framework is cooperative. As shown in Figure 5 such a cooperative arrangement results in a compensation of their electric dipoles, except along the *a*-axis. But as this compound crystallizes in a racemic mixture and the two enantiomers show an arrangement of the DMA cations in opposite directions (cf. Figures 5a) and 5b)), the final result would be a compensation of the electric dipoles also along the *a*-axis, so that an antiferroelectric behavior would be expected at low temperature.

Additional studies, including the measurement of P(E) curves, are still necessary to unambiguously confirm the antiferroelectric nature of the low temperature phase.

In summary, we deepened the understanding of the origin of the disorder−order transition that takes place in $Mn(HCOO)_3[(CH_3)_2NH_2]$ and that gives rise to the marked dielectric transition. It is caused by the freezing of the molecular rotation of the DMA cations, that is present at higher temperatures, giving rise to a cooperative ordering of the DMA cations inside the Mn-formate framework because of the formation of permanent N−H···O bonds between the DMA cations and the formate anions.

In any case, the mechanism of the transition would be more complex than that of a simple and homogeneous 3-fold order−disorder model as its associated entropy has been reported to be almost 1 order of magnitude lower than that expected for the former.[16]

Acknowledgment. The authors are grateful for financial support from Xunta de Galicia under projects PGIDIT06PXB103298PR and INCITE08E1R103068ES. M.S.-A. acknowledges Xunta de Galicia for support under Parga Pondal program, M.A.S.-R. the Spanish Ministerio de Ciencia e Innovación for the Grant "Estancias de Profesores e Investigadores Seniors en Centros Extranjeros" PR2008-0315, and J.S. thanks M. Jansen and the Max-Planck Institute for Solid State Research of Stuttgart for a fellowship. They also thank A. Fernandez Lopez for his help with the structure refinement, M. Jansen for the access to the Raman and IR equipments in the Max-Planck Institute for Solid State Research of Stuttgart, and A. Schulz for collecting the Raman spectra.

Supporting Information Available: X-ray crystallographic information files (CIF) for crystal structure at $T = 295$ K and $T = 100$ K. Figure S1: DSC results. Figure S2: IR spectra. Figure S3: proposed rotation of the DMA cations inside the Mn-formate framework. Table IV: observed frequencies in cm^{-1} of the vibrational spectra and suggested assignments. This material is available free of charge via the Internet at http://pubs.acs.org.